JOURNAL OF AGRICULTURAL AND FOOD CHEMISTRY
ARTICLE

J. Agric. Food Chem. 2010, 58, 1523–1534 1523
DOI:10.1021/jf9032602

Green Tea Catechins and Their Oxidative Protection in the Rat Eye

Kai On Chu,[†,‡] Kwok Ping Chan,[†] Chi Chiu Wang,[‡] Ching Yan Chu,[‡] Wai Ying Li,[†] Kwong Wai Choy,[‡] Michael Scott Rogers,[‡] and Chi Pui Pang*[,†]

[†]Department of Ophthalmology and Visual Sciences, The Chinese University of Hong Kong, Hong Kong Eye Hospital, Kowloon, Hong Kong, and [‡]Department of Obstetrics and Gynecology, Prince of Wales Hospital, Shatin, New Territories, Hong Kong.

Catechins, active constituents of green tea, are well-known antioxidative natural products. It was proposed that green tea extract (GTE) consumption could benefit the eye, and the pharmacokinetics of catechins and oxidation status in rat eye were investigated after oral administration. Sprague−Dawley rats were fed GTE and sacrificed at different time intervals. Their eyes were dissected into cornea, lens, retina, choroid-sclera, vitreous humor, and aqueous humor for analysis of catechins and 8-epi-isoprostane by HPLC-ECD and GC-NCI-MS, respectively. Catechins were differentially distributed in eye tissues. Gallocatechin was present at the highest concentration in the retina, 22729.4 ± 4229.4 pmol/g, and epigallocatechin in aqueous humor at 602.9 ± 116.7 nM. The corresponding area-under-curves were 207,000 pmol × h/g and 2035.0 ± 531.7 nM × h, respectively. The time of maximum concentration of the catechins varied from 0.5 to 12.2 h. Significant reductions in 8-epi-isoprostane levels were found in the compartments except the choroid-sclera or plasma, indicating antioxidative activities of catechins in these tissues.

KEYWORDS: Green tea; catechins; eye tissues; pharmacokinetics; distribution

INTRODUCTION

Oxidative stress, principally through the effects of reactive oxygen species and oxidative free radicals, causes biological disturbances such as DNA damage and activation of proteolytic enzymes that lead to tissue cell damage or dysfunction as seen in the pathogenesis of many ophthalmic diseases. Photooxidative stress can inactivate catalase in the lens to initiate cataract formation (*1*). Long-term effects of reactive oxygen intermediates could damage retinal tissue cells, especially photoreceptor cells, retinal pigment epithelium, and choriocapillaries (*2*). Oxidation is also associated with primary open angle glaucoma (POAG). Oxidative stress may also exert direct cytotoxic effects and cause retinal ganglion cell death (*3*). It may also cause damage to the trabecular meshwork and lead to elevation of intraocular pressure due to obstruction of aqueous humor outflow (*4*). Oxidative stress is responsible for retinopathy in preterm neonates (*5*).

Various antioxidants have been examined for protection against oxidative stress in the eye, such as vitamin C, vitamin E, lutein, and zeaxanthin, although the results are not consistent (*6*−*8*). Green tea, a beverage consumed by humans for thousands of years with well-known safety, is known for its antioxidative activities in many biological systems (*9*). Tea polyphenols such as epigallocatechin gallate (EGCG) possess many cytoprotective properties such as inhibition of pro-inflammatory cytokines and inhibition of growth factors inducing neovascularization (*10*). Green tea therefore appears to be a good candidate for eye protection. The principal tea polyphenols, catechins, have been tested in vitro for various ophthalmologic treatments under induced oxidative challenge (*11*). In a pharmacokinetic study we have shown that in pregnant rats fed green tea extract (GTE) catechins are distributed to the placenta and fetal tissues (*12*). Although maternal plasma total catechin levels were tens of times higher than fetal levels, (−)-epigallocatechin gallate (EGCG) concentration was higher in the fetus than in maternal plasma. In the fetus, the absorbed catechins were found in the brain, eye, heart, lung, kidney, liver, and placenta, with catechin gallates more effectively taken up by fetal organs than catchins (*13*).

Catechins belong to the flavan-3-ol group of chemicals. They exist as different diastereomers called epimers and their related gallic acid esters. When an additional hydroxyl group attaches to the dihydroxybenzyl B ring to form a 3′,4′5′-trihydroxybenzyl moiety, it is a gallo derivative. When a trihydroxyphenolic moiety, gallic acid, attaches to the hydroxyl group of flavane to form an ester, it is called a gallate compound. Depending on the steric direction of attachment of the B ring and gallate moiety, epi- or non-epi-isomers are formed. For the (−)-epi-isomer, the absolute configuration is 2*R*:3*R*, whereas the (+)-epi-isomer has the configuration 2*S*:3*S*. On the other hand, the absolute configuration of the (−)-non-epi-isomer is 2*S*:3*R*, whereas that of the (+)-non-epi-isomer is 2*R*:3*S*. Different isomers possess their own characteristic absorption patterns, antioxidative properties, and biological acitivities.

*Address correspondence to this author at the Department of Ophthalmology and Visual Sciences, The Chinese University of Hong Kong, 3/F, Hong Kong Eye Hospital, 147K Argyle Street, Kowloon, Hong Kong [telephone (852) 27623169; fax (852) 27159490; e-mail cppang@cuhk.edu.hk].

Published on Web 01/19/2010

Green tea consumption could benefit the eye against oxidative stress if the green tea catechins can penetrate into eye tissues. In this study, we investigated the uptake and distribution of catechins and their gallates in eye tissues and fluids in rats fed orally with GTE. We also examined their effects on the levels of 8-epi-isoprostane (8-iso-$PGF_{2\alpha}$), an in vivo biomarker for physiological oxidative stress (*14*), to assess its antioxidative properties.

MATERIALS AND METHODS

Materials and Reagents. (+)-Catechin (C), (−)-epicatechin (EC), (−)-gallocatechin (GC), (−)-epigallocatechin (EGC), (−)-catechin gallate (CG), (−)-epicatechin gallate (ECG), (−)-gallocatechin gallate (GCG), (−)-epigallocatechin gallate (EGCG), β-D-glucuronidase (G-0251), sulfatase (S-9754), ascorbic acid, uric acid, and reduced glutathione (GSH) were from Sigma Chemical Co. (St. Louis, MO). Sodium dithionite was obtained from RDH (Seelze, Germany). Oasis HLB 30 mg columns were from Waters (Milford, MA). Other reagents and solvents were obtained in their highest grade available from BDH (Poole, U.K.). A standard stock mixture of C, EC, GC, EGC, ECG, GCG, and EGCG at 100 μg/mL each was prepared in ascorbic acid−EDTA (0.2% ascorbic acid/0.1% EDTA in 0.4 M phosphate buffer, pH 3.6) and stored in small aliquots at −80 °C until use. Decaffeinated GTE, Sunphenon DCF-1, was a gift from Taiyo Kagaku Co. Ltd. (Tokyo, Japan). Each 166 mg of GTE contained 53.6 mg of EGCG, 24.8 mg of ECG, 24.2 mg of GCG, 21.6 mg of EC, 17.6 mg of EGC, 17.0 mg of GC, and 7.2 mg of C.

8-Isoprostaglandin $F_{2\alpha}$-D_4 (8-iso-$PGF_{2\alpha}$-D_4), 8-iso-$PGF_{2\alpha}$, and other prostaglandin metabolites were from Cayman (Ann Arbor, MI). Bis-(trimethylsilyl)trifluoroacetamide (BSTFA), pentafluorobenzyl bromide (PFBBr), *N*,*N*-diisopropylethylamine, and dodecane were purchased from Sigma. Butylated hydroxytoluene (BHT) was from Calbiochem (La Jolla, CA). Triphenylphosphine was from Aldrich (Milwaukee, WI). Acetonitrile (HPLC grade) was obtained from BDH. Absolute ethanol, potassium hydroxide, hydrochloric acid (33%), citric acid, cyclohexane, and ammonia (25%) at their highest purity grade were obtained from RDH. Octadecyl silica (ODS) 500 mg cartridges (Discovery DSC-18LT) were from Supelco (Bellefonte, PA). Water purification was carried out on a Milli-Q purification system from Millipore (Molsheim, France).

Animal Treatment. Eleven groups of Sprague−Dawley rats, each weighing about 200 g and aged 9 weeks, were obtained from the animal house of the Chinese University of Hong Kong. Each group contained six rats. Ethics approval for the study was obtained from the Animal Ethics Committee of the University. Dams were housed at 25 °C with a 12 h light and dark cycle with free access to chow and water for 7 days. They were then fasted overnight and weighed before the experiments. GTE tablets were powdered and suspended in 0.5 mL of water. Previous studies on the pharmacokinetics of catechins in rats have used a wide range of EGCG dosages from 25 to 500 mg/kg (*15*, *16*). In this study, similar to our previous studies (*12*, *13*), we used 550 mg/kg GTE. The doses of catechins were comparable to most published reports: 178 mg/kg EGCG, 82.7 mg/kg ECG, 80.7 mg/kg GCG, 72.0 mg/kg EC, 58.7 mg/kg EGC, 56.7 mg/kg GC, and 24 mg/kg C. The rats were randomly assigned to 11 groups, namely, 0, 0.5, 1, 2, 3, 5, 8, 10, 12, 16, and 20 h. The dams from each time point were fed 0.5 mL of GTE suspension with a feeding tube. After anesthetization with 200 mg/kg ketamine and 40 mg/kg xylazine mixture IM, the rats were sacrificed at various time points after GTE administration. Rats of time zero were immediately sacrificed after feeding and anesthetization. Another six dams were fed 0.5 mL of water without GTE as negative controls. The eyes were enucleated. The aqueous and vitreous humors, cornea, lens, retina, and choriod-sclera were dissected out immediately. Tissues were thoroughly washed in ice-cold saline to remove any catechins adhering on the tissue surface. All were snap-frozen in liquid nitrogen and stored at −80 °C. Plasma was obtained from peripheral whole blood after centrifugation at 3000 rpm at 4 °C for 10 min (*17*, *18*) and stored at −80 °C.

Tissue and Plasma Assays for Catechins. Tissue preparation and analysis followed a published fully validated method (*17*). The weighed tissues were homogenized in 0.25 mL of methanol/ethyl acetate (2:1) and 0.25 mL of 0.3 M sodium dithionite with 0.1% w/v Na_2EDTA in ice. After centrifugation at 10000*g* at 4 °C, the supernatant was purged by nitrogen to remove the organic solvents and reduce the volume to about 0.2 mL. Then 0.25 mL of 0.4 M phosphate buffer (pH 6.8) and 20 μL of a mixture of β-D-glucuronidase (2500 U) and sulfatase (1 U) were added for digestion of the conjugated catechins by incubation of the mixture at 37 °C for 45 min.

The extraction was performed using a modified plasma extraction method (*18*). The thawed plasma or humor was mixed with 40 μL of ascorbate-EDTA buffer solution, 40 μL of 0.4 M NaH_2PO_4 buffer (pH 7.4), and 20 μL of a mixture of β-D-glucuronidase (250 U) and sulfatase (1 U). After purging by nitrogen and incubation at 37 °C for 45 min, it was snap-cooled in ice prior to the addition of 1 mL of 0.05 M NaH_2PO_4 buffer (pH 7.0) and solid phase extraction with elution by 10 mL of a methanol/ethyl acetate (2:1) mixture at 35 °C into a tube containing 20 μL of 2% ascorbate−EDTA to protect the catechins against oxidation. After evaporation, it was dissolved into 100 μL of a mixture containing 10% acetonitrile and 0.06% trifluoroacetic acid in 0.05 M phosphate buffer (pH 3.0) and filtered for analysis by HPLC.

Assay for 8-Iso-$PGF_{2\alpha}$ in Ocular Tissues and Fluids. The protocol was based on published validated methods (*19*, *20*). In brief, vitreous and aqueous were extracted with ice-cold Folch solution (chloroform/methanol, 2:1 v/v) containing 0.005% BHT and TPP. After precipitation by $MgCl_2$, the organic layer was removed and dried under nitrogen. Ocular tissues were homogenized in ice-cold Folch solution, given 0.5 mL of 0.9% sodium chloride to remove water-soluble compounds and protein residues, and centrifuged. The organic layer was taken out and dried under nitrogen. The organic residues of the ocular fluid or tissues were hydrolyzed by KOH (15%) for 30 min at 37 °C. After acidification by HCl to pH 3, 8-iso-$PGF_{2\alpha}$ was extracted by C18 and silica Sep-Pak, derivatized with PFBB, and purified by TLC. The isoprostane residues were scraped out, extracted by ethyl acetate, and derivatized by BSTFA, then dried and dissolved in dodecane for GC-NCI-MS analysis.

Pharmacokinetic and Data Analyses. The pharmacokinetic parameters of catechins were analyzed by WINNONLIN Professional version 4.01. To identify the average time a molecule stayed in eye tissues, predicted mean residence time from zero time point to infinity (MRT_{inf}) was obtained from the predicted area under the first moment curve ($AUMC_{inf}$ in pmol × h^2/L) divided by the predicted area under the curve from zero time point to infinity (AUC_{inf} in pmol × h/L). The parameters, MRT_{inf}, maximum peak time (T_{max}), maximum concentration (C_{max}), area under curve (AUC), terminal elimination rate (λ_z), oral clearance (Cl/F), and volume of distribution (V_z), were evaluated by noncompartmental models. The means of T_{max}, C_{max}, and AUC were compared by nonparametric analysis using the Kruskal−Wallis H method. The Student *t* test was used for comparing the means of each catechin gallate with corresponding catechins, between epimer with corresponding nonepimer, and the isoprostane levels of each humor and tissue at zero time with the first minimum level. Correlations between exposure level, AUC, and elimination rate, λ_z, and between the AUC and MRT in each tissue were assessed by linear regression.

All of the statistical analyses were performed by SPSS 15.0. To compare the uptake and exposure of each catechin, normalized AUC for plasma and relative AUC for humors and eye tissues were plotted. Normalized AUC of each catechin was computed as AUC (nM × h) of plasma divided by the labeled dose (mol) in the green tea extract. The unit of normalized AUC was h/L × 10^{-3} in plasma. The equation for normalized AUC (*12*) is

$$\text{normalized AUC (plasma)} = \frac{\text{AUC (plasma)}}{\text{labeled dose (GTE)}}$$

The relative AUC values of catechins in humors (nM × h) and eye tissues were computed as AUC (pmol × h/g) of each catechin in tissues divided by AUC of the catechin in plasma:

$$\text{relative AUC (humor/tissues)} = \frac{\text{AUC (humor/tissues)}}{\text{AUC (plasma)}}$$

The relative AUC for humor has no unit, whereas relative AUC for eye tissue is expressed as mL/g.

RESULTS

Catechins and Cathechin Gallates. The catechin concentration versus time profiles in plasma appeared as single peaks, whereas

in humors and eye tissues they appeared as multiple peaks (**Figure 1**). Some catechins remained at high levels even after 20 h of administration, for example, GC in vitreous humor and in choroid-sclera. No catechin was detected in any of the tissues and fluids in the negative control group. Also, shapes of the profiles of catechins and catechin gallates were in general similar in all compartments except the catechins in the lens and ECG in the cornea. Furthermore, the profiles between catechins and catechin gallates within the same compartment were different. GC levels in the eye compartments were the highest except in the aqueous humor and cornea.

Table 1 shows the pharmacokinetic parameters. In general, C_{max} values of catechins were lower in both humors than in plasma except GC, which was slightly higher in vitreous humor than in plasma. No GC was found in aqueous humor. EGC and EC were dominantly present in plasma, and GC and C were predominant in vitreous humor, whereas the EGC level was higher in aqueous humor. GC and EGC were dominant in all eye tissues except the cornea, where GC was absent. GC and EGC levels were 3−4600 times higher than other catechins in the same tissue. Furthermore, the C_{max} levels of GC and EGC in retina were 10−250 times higher than in plasma. Similarly, the exposure levels of GC and EGC, as revealed by AUC, dominated in the tissues, at 3−50000-fold higher than other catechins in the same tissue. In general, large volumes of distribution, based on terminal phase V_z, of EGC and EGCG were found in aqueous and vitreous humor, whereas GC, C, and GCG were highest in plasma. Although only one catechin, GCG, had a very large oral clearance, Cl/F, in plasma, two catechins, EGC and ECG, were found higher in aqueous humor and three, EGC, ECGC, and ECG, in vitreous humor. EGCG and GCG possessed very high oral clearance in eye tissues.

After the AUC was normalized according to applied dose, some isomers were dominant in plasma. The normalized AUC levels of epimers were higher than those of nonepimers. Also, non-gallate catechin levels appeared to be higher than gallate derivatives. **Figure 2a** shows that the normalized AUC values of EGC and EC were dominant in plasma. This phenomenon was similar to the C_{max} in plasma. The relative AUC values of nonepimers were dominant in vitreous humor, but no obvious difference existed between gallates and non-gallates. These could be observed from the dominating GC, C, and GCG. Also, their relative exposure levels were higher than 1 (**Figure 2b**). In aqueous humor, no trend of relative AUC domination for the epimers and gallates was found. There was no epimer or gallate preference in the eye tissues except in the cornea, where gallate derivatives were slightly favored. The level of GC was highly dominant in all eye tissues except the cornea, where instead the GCG level was dominant (**Figure 2c**).

No inverse relationship existed between the level of catechin exposure, AUC, and the elimination rate, λ_z, nor was there a positive association between the AUC and mean residence time, MRT_{inf} except in the choroid-sclera, where a good correlation was found between AUC and MRT_{inf} ($R = 0.9859$, $p < 0.001$) (**Table 2**).

T_{max} of catechins varied within each fluid and tissue; for example, T_{max} of GC in retina varied from 1 h for GC to 10 h for EGCG (**Table 1**). The T_{max} of each catechin varied across fluids and tissues; for example, T_{max} of EGCG varied from 0.5 h in plasma to 10 h in retina, giving three general trends of T_{max} patterns (**Figure 3**). GC showed a general increasing trend from the plasma via outer choroid-sclera, posterior segment to the anterior segment. GC, EGC, EC, and EGCG displayed a middle puddle appearance, whereas GCG and ECG exhibited a flat platform with a sharp rise in the anterior region.

Assay for 8-Epi-isoprostane. 8-Epi-isoprostane levels were significantly decreased in the aqueous humor, vitreous, cornea, and lens ($p < 0.001$, $n = 6$) after ingestion of green tea extract. Low levels of isoprostane were maintained throughout the study period. The isoprostane level slowly but significantly decreased in the retina ($p < 0.05$, $n = 6$), but its level gradually increased back to the original. No significant decrease in 8-epi-isoprostane level was observed in plasma and choroid-sclera (**Figure 4**).

DISCUSSION

Although many antioxidants have been studied in the eye (*6*−*8*), to the best of our knowledge this is the first paper to show distribution of individual catechins after ingestion of green tea extract and to evaluate their in vivo antioxidative effects in various parts of the mammalian eye. Because multicatechin profile studies on eye tissues are lacking, we can only compare the EGCG level in the brain with the level in our retina data to support our study. Because the blood−brain barrier is similar to the blood−retinal barrier, this comparison seems to be reasonable. About 0.5 nmol/g EGCG was found in the brain after oral administration of 500 mg/kg EGCG (*16*), whereas a similar level, 0.73 nmol/g EGCG, was found in retina after adjusting for our different applied EGCG dose.

As in our previous study (*13*), we used β-D-glucuronidase and sulfatase to convert the main metabolites to their parental compounds. Therefore, we measured total catechins instead of free or conjugated catechins for analysis. Because there are many different forms of conjugates, to simplify our analysis for the whole range of catechins, we used total catechins for distribution analysis. In fact, the major conjugates of catechins in plasma are 5-*O*-β-glucuronides that retain the antioxidative properties of their parental compounds (*21*, *22*).

Multiple peaks were exhibited in the humors and in the eye tissues (**Figure 1**), indicating that the catechins or their metabolites may be recirculated or reabsorbed into the compartments, and their levels were maintained during the study period. The levels of some catechins might be sustained at high levels until the end of the study. This phenomenon was also found in our previous study in fetal eye (*13*). Similar shapes of the profiles of the catechins and catechin gallates in a compartment suggested similar absorption mechanisms between them within the same compartment. Different profile shapes found between catechins and catechin gallates within the same compartment indicated different absorption mechanisms. Similarly, some unique profiles appearing even within catechins or catechin gallates in the same compartment such as ECG in the cornea suggested the absorption mechanism might be different. Some catechins, especially the gallate derivatives EGCG and GCG, were not retained in some compartments (**Figure 1d**−**g**) but showed abrupt sharp peaks in the time profile. This indicated they may be highly conjugated after absorption, limiting the retention in tissue cells (*23*).

It has been found that catechins are selectively absorbed into the body compartments. The total AUC of EGC and EC was higher than that of EGCG in plasma even though the dose was < 20% that of EGCG (*24*). In our previous studies, we also found that catechins were differentially absorbed into maternal plasma and various fetal organs (*12*, *13*). In this study, we also found similar situations in different eye compartments (**Figure 2**). The levels of GC and EGC in retina were 88- and 31-fold higher than the EGCG level (**Figure 1**; **Table 1**), although their applied doses were 2 to 3 times lower. This suggests that GC and EGC can selectively pass through the blood−retinal barrier. In fact, GC and EGC were predominately retained in the eye tissues and vitreous humor when considering the relative AUC (**Figure 2**).

(a) Plasma

Catechin as a group

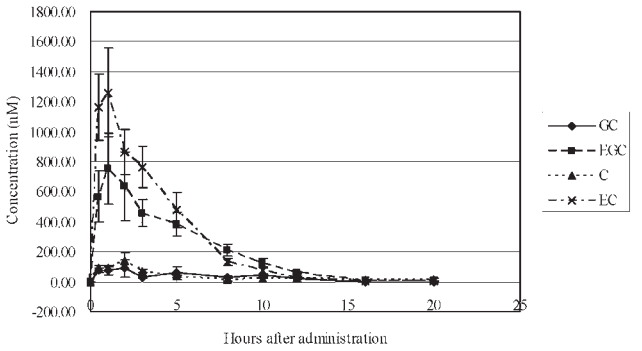

Catechin gallate as a group

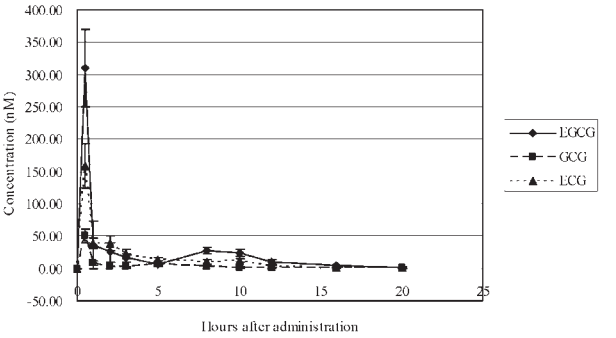

(b) Aqueous humor

Catechin as a group

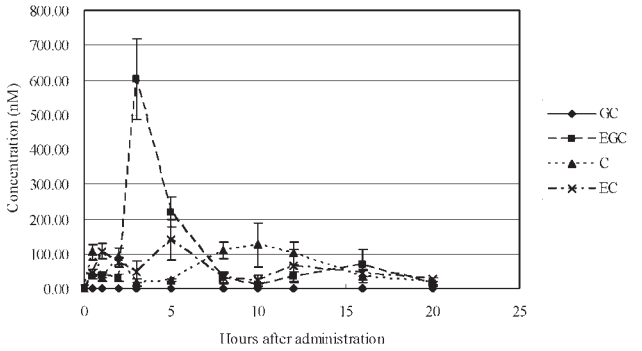

Catechin gallate as a group

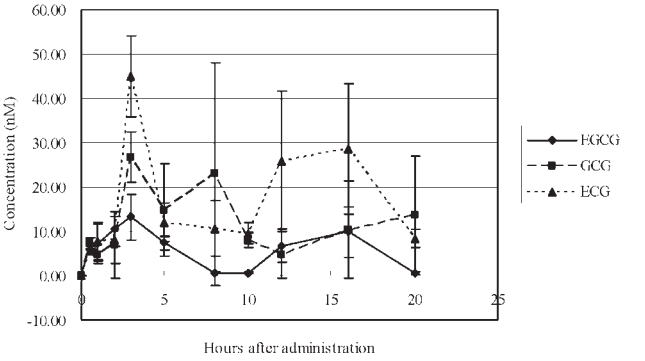

(c) Vitreous humor

Catechin as a group

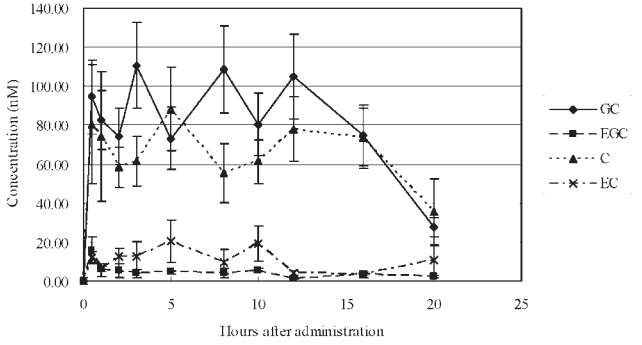

Catechin gallate as a group

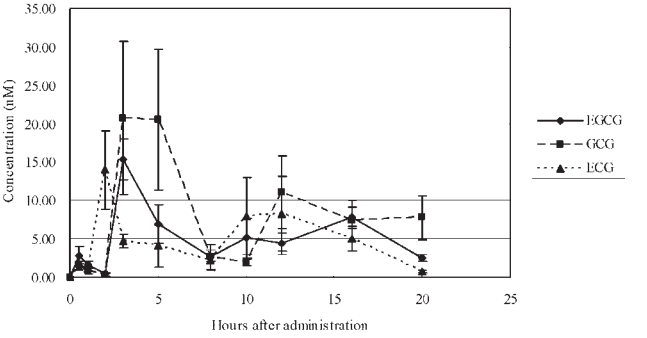

(d) Choroid-Sclera

Catechin as a group

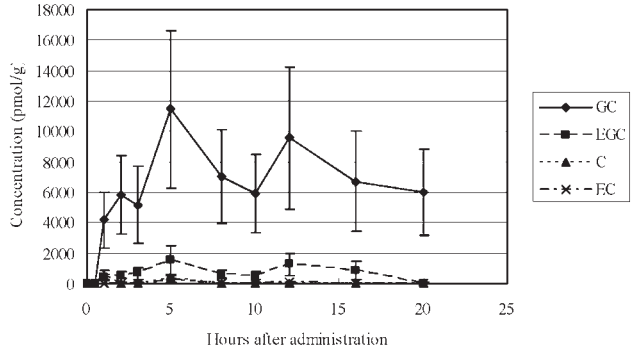

Catechin gallate as a group

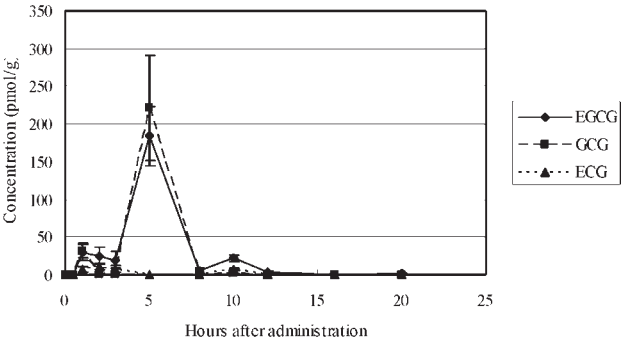

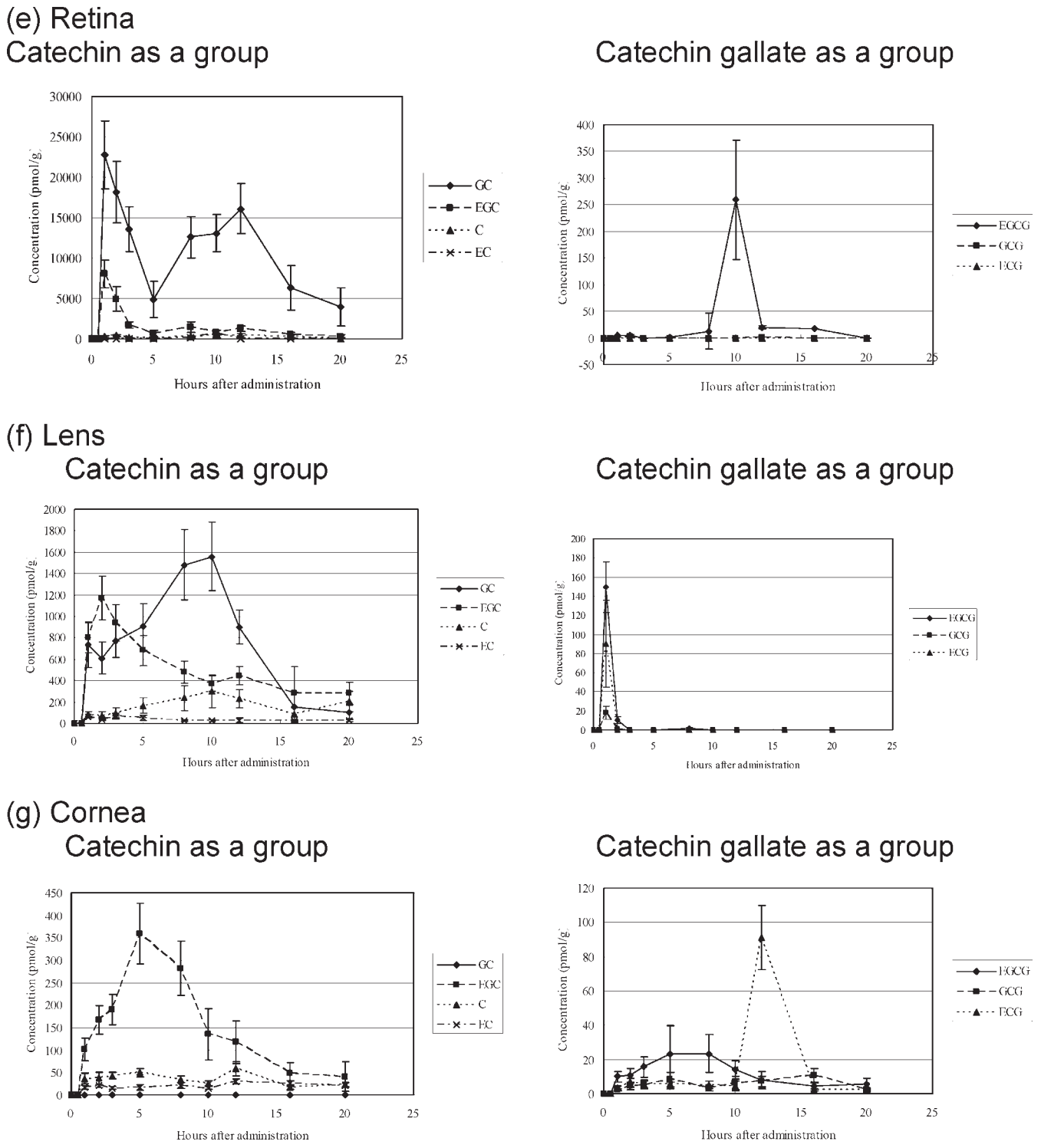

Figure 1. Profiles of total catechins and their gallate esters (free and conjugated) changes: (**a**) plasma; (**b**) aqueous humor; (**c**) vitreous humor; (**d**−**g**) various eye tissues after 550 mg/kg GTE treatment ($n = 6$). The profiles in the compartments were divided into two groups according to the presence of gallate derivatives. Error bars represent standard derivation.

However, the anterior segment of the eye appeared not to retain GC. The absence of GC in the cornea and aqueous humor might indicate either its transferring pathway was blocked in the entire anterior segment or it was unable to enter the aqueous humor, thus preventing its transfer to the cornea. Chow et al. (*24*) applied Polyphenon E, a green tea extract containing 600 mg of EGCG, to human subjects and found that EGC and EC were mainly converted to water-soluble metabolites, glucuronide and sulfate conjugates, in the plasma. This explains why the total EGC and EC levels in our study were higher in the aqueous than vitreous humor because the aqueous humor is an open watery draining system compared to the vitreous humor.

Disequilibrium in the absorptions of catechins may involve selective ocular tissue protein binding rather than passive diffusion (*15*, *25*). The bipolar functional groups of EGCG may prevent it from penetrating into the blood−brain barrier (*15*). Active absorption mechanisms, which are commonly found in ocular drug deliveries, might also be involved (*26*), as shown by

Table 1. Pharmacokinetic Parameters of Catechins in Eye Tissues 20 h after a Single Dose of 550 mg/kg Sunphenon DCF-1 Green Tea Extract Administered Orally to Rats

parameter	GC	EGC	C	EC	EGCG	GCG	ECG
T_{max} (h)							
plasma	0.8 ± 0.6	0.5 ± 0.1	2.0 ± 0.2*[a]	0.8 ± 0.1	0.5 ± 0.0	0.5 ± 0.1	0.5 ± 0.1
aqueous humor	−[b]	3.0 ± 0.1	8.3 ± 0.8*	5.0 ± 0.1*	2.8 ± 0.1	3.8 ± 2.0	3.0 ± 0.4
vitreous humor	3.2 ± 0.2	0.5 ± 0.1	4.3 ± 1.6	5.0 ± 0.2*	3.1 ± 0.2	3.5 ± 0.2	2.0 ± 0.2
choroid-sclera	5.1 ± 0.1	5.2 ± 0.2	5.1.0 ± 0.2	5.1 ± 0.1	5.0 ± 0.2	5.0 ± 0.1	2.0 ± 0
retina	1.0 ± 0.1	1.2 ± 0.1	3.7 ± 4.1	10.2 ± 0.2*	10.1 ± 0.1*	2.0 ± 0.1	−
lens	10.1 ± 0.2*	1.4 ± 0.1	10.1 ± 0.3*	2.8 ± 0.3	1.0 ± 0.1	1.0 ± 0.1	1.0 ± 0.1
cornea	−	4.9 ± 0.3	12.1 ± 0.3	12.2 ± 0.3	7.5 ± 1.2	16.1 ± 0.3*	12.1 ± 0.2
C_{max} (nM)							
plasma	91.5 ± 57.4	754.9 ± 235.8	139.0 ± 57.0	1258.4 ± 294.0*	310.4 ± 59.9	50.8 ± 10.4	159.1 ± 33.9
aqueous humor	−	602.9 ± 116.7*	127.4 ± 62.8	138.9 ± 58.5	13.2 ± 5.1	33.5 ± 20.4	47.8 ± 8.1
vitreous humor	110.6 ± 22.1*	15.9 ± 7.0	96.5 ± 23.3*	20.5 ± 10.6	15.4 ± 2.7	20.9 ± 9.9	14.0 ± 5.1
C_{max} (pmol/g)							
choroid-sclera	11461.8 ± 5168.7*	1506.3 ± 941.1	477.6 ± 346.9	283.5 ± 66.5	184.4 ± 39.0	220.5 ± 69.7	10.7 ± 4.3
retina	22729.4 ± 4229.4*	8020.8 ± 1658.49*	492.7 ± 235.2	608.0 ± 112.0	259.1 ± 67.2	3.2 ± 1.9	−
lens	1558.1 ± 318.4*	1172.3 ± 207.8*	300.0 ± 151.5	72.3 ± 19.1	149.1 ± 26.5	18.0 ± 6.6	90.3 ± 45.8
cornea	−	359.4 ± 66.8*	58.5 ± 15.4	30.6 ± 5.7	25.2 ± 15.5	10.7 ± 3.9	91.1 ± 18.7
AUC (nM × h)							
plasma	547.8 ± 240.7	4096.8 ± 975.1*	645.6 ± 193.3	5272.9 ± 1072.5*	420.7 ± 117.7	68.2 ± 15.0	283.5 ± 66.3
aqueous humor	−	2035.0 ± 531.7*	1255.1 ± 423.7	1156.2 ± 459.8	121.2 ± 53.0	248.0 ± 192.2	382.2 ± 171.2
vitreous humor	1634.2 ± 332.2*	79.2 ± 30.2	1404.9 ± 251.2*	205.8 ± 97.4	109.5 ± 27.4	172.7 ± 70.3	100.8 ± 47.1
AUC (pmol × h/g)							
choroid-sclera	142276.7 ± 66344.8*	15322.9 ± 9030.6*	1563.8 ± 981.0	968.2 ± 285.8	607.8 ± 150.6	580.2 ± 183.0	34.2 ± 15.0
retina	206683.5 ± 48654.4*	26793.3 ± 8889.2*	4904.4 ± 2704.0	1463.1 ± 296.3	652.4 ± 193.3	4.4 ± 2.7	−
lens	14907.7 ± 3384.4*	9838.9 ± 2484.5*	3319.4 ± 1606.5	681.1 ± 218.7	125.1 ± 22.9	14.6 ± 5.5	22.6 ± 11.4
cornea	−	3027.2 ± 772.7*	678 ± 153.2	417.9 ± 99.7	239.4 ± 122.4	124.61 ± 55.0	339.7 ± 82.3
λ_z (h^{-1})							
plasma	0.107 ± 0.010	0.213 ± 0.015	0.104 ± 0.038	0.371 ± 0.000*	0.236 ± 0.007	0.171 ± 0.013	0.211 ± 0.010
aqueous humor	−	0.045 ± 0.001	0.209 ± 0.012	0.093 ± 0.062	0.304 ± 0.012*	0.111 ± 0.033	0.124 ± 0.043
vitreous humor	0.166 ± 0.010	0.041 ± 0.001	0.106 ± 0.030	0.067 ± 0.004	0.058 ± 0.012	0.042 ± 0.006	0.224 ± 0.035*
choroid-sclera	0.057 ± 0.001	0.461 ± 0.015	0.220 ± 0.014	0.488 ± 0.007	0.267 ± 0.019	0.929 ± 0.049*	−
retina	0.188 ± 0.045	0.203 ± 0.050	0.245 ± 0.010	2.432 ± 0.154*	0.413 ± 0.040	−	−
lens	0.302 ± 0.049*	0.084 ± 0.020	0.234 ± 0.032	0.049 ± 0.004	0.269 ± 0.011	3.16 ± 0.13	−
cornea	−	0.170 ± 0.031	0.116 ± 0.007	0.043 ± 0.012	0.125 ± 0.001	0.372 ± 0.006	0.477 ± 0.021*
MRT_{inf} (h)							
plasma	9.5 ± 0.8*	4.7 ± 0.2	11.0 ± 9.5	3.3 ± 0.0	5.4 ± 0.2	4.8 ± 0.2	4.1 ± 0.2
aqueous humor	−	21.1 ± 0.1*	10.4 ± 0.5	15.0 ± 2.8	9.3 ± 0.4	12.6 ± 5.2	13.8 ± 0.7
vitreous humor	11.0 ± 0.2	23.1 ± 1.0	15.1 ± 4.8	15.9 ± 0.8	19.0 ± 2.3*	26.8 ± 2.6	10.2 ± 0.2
choroid-sclera	21.5 ± 0.3*	9.5 ± 0.2	6.1 ± 0.1	6.6 ± 0.3	5.3 ± 0.0	4.9 ± 0.0	−
retina	10.5 ± 1.9	7.2 ± 1.7	11.0 ± 0.7*	9.7 ± 0.1	10.6 ± 0.2	−	−
lens	8.6 ± 0.4	13.6 ± 5.1	11.2 ± 0.4	21.1 ± 1.5*	1.8 ± 0.1	1.25 ± 0.0	−
cornea	−	8.7 ± 1.5	12.8 ± 0.3	32.0 ± 12.9*	10.4 ± 0.0	11.6 ± 0.2	11.3 ± 0.1
Cl/F (L/h)							
plasma	93.8 ± 35.8	14.7 ± 3.6	35.6 ± 13.6	14.6 ± 3.2	289.7 ± 76.5	778.3 ± 186.3*	204.4 ± 49.6
aqueous humor	−	482.7 ± 143.3	20.0 ± 0.5.9	52.5 ± 13.6	1068.8 ± 346.7*	197.8 ± 91.1	122.4 ± 40.0
vitreous humor	32.0 ± 6.9	460.2 ± 132.0	14.5 ± 4.0	239.1 ± 84.3	788.9 ± 169.0*	160.6 ± 44.9	609.8 ± 201.1
Cl/F (kg/h)							
choroid-sclera	0.8 ± 0.3	14.6 ± 5.4	65.5 ± 24.6	282.3 ± 76.8	439.2 ± 109.7*	213.6 ± 60.0	−
retina	0.8 ± 0.2	7.2 ± 2.3	19.6 ± 7.1	181.7 ± 40.1	395.9 ± 112.4*	−	−
lens	12.4 ± 3.0	15.0 ± 4.8	23.4 ± 8.2	219.1 ± 53.0	1987.0 ± 406.7	8640164 ± 262645*	−
cornea	−	61.0 ± 17.4	101.5 ± 23.1	289.8 ± 104.2	1045.3 ± 366.6*	988.7 ± 320.5	387.3 ± 95.6
V_z (L)							
plasma	860.1 ± 294.7	69.9 ± 19.4	359.2 ± 79.8	39.4 ± 8.7	1235.3 ± 344.7	4534.5 ± 920.8*	966.4 ± 210.9
aqueous humor	−	10583.8 ± 3032.9*	94.8 ± 25.4	714.7 ± 312.3	3546.4 ± 1209.1	1673.0 ± 556.9	1080.5 ± 425.6
vitreous humor	193.6 ± 47.0	11326.4 ± 3403.5	139.8 ± 21.7	3630.6 ± 1362.4	14096.0 ± 4220.5	3920.2 ± 1318.4*	2842.8 ± 1094.4
choroid-sclera	n/a[c]	n/a	n/a	n/a	n/a	n/a	n/a
retina	n/a	n/a	n/a	n/a	n/a	n/a	n/a
lens	n/a	n/a	n/a	n/a	n/a	n/a	n/a
cornea	n/a	n/a	n/a	n/a	n/a	n/a	n/a

[a] * indicates that the catechin(s) has significant higher ($p < 0.05$, $n = 6$) level of the parameter in the corresponding biological fluid or tissue than the others. [b] −, data cannot be determined. [c] n/a, not applicable.

the nonsynchronized profiles in that single peaks appeared in the plasma but multiple peaks in the humors and eye tissues (**Figure 1**). Second, different catechins dominated in different tissue compartments, thus indicating discriminative distributions. GC and EGC were dominant in choroid-sclera, retina, and lens, but EGC and EC were dominant in plasma and aqueous humor. Tissue and vitreous levels of some catechins were higher than in plasma. GC was absent in aqueous humor. The AUC values of

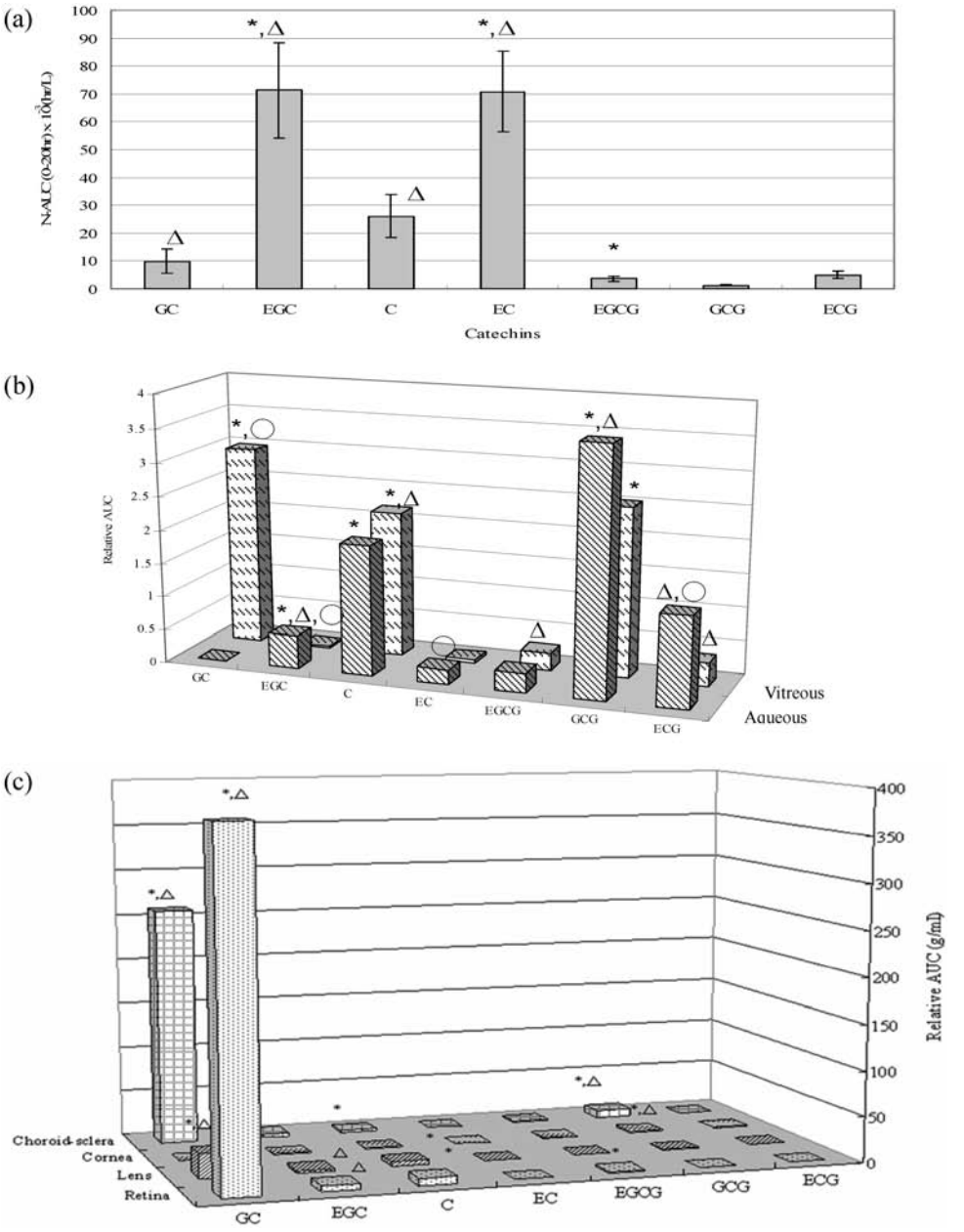

Figure 2. Normalized relative AUC levels of total catechins (conjugated and free form) in ocular fluid and tissues: (**a**) AUC levels of different catechins in plasma after normalization by the corresponding dose in the GTE; (**b**) relative AUC levels of catechins in vitreous and aqueous humor; (**c**) relative AUC levels of catechins in retina, lens, cornea, and choroids-sclera. The levels of AUC were calculated from 0 to 20 h. Error bar represented standard derivation. ∗, the level of an epimer was significantly higher than the corresponding nonepimer or vice versa in the same compartment ($p < 0.05$, $n = 6$); Δ, the level of a catechin was significantly higher than the corresponding gallate derivative or vice versa in the same compartment ($p < 0.05$, $n = 6$); ○, the level of one of the catechins was significantly higher in one humor than in the other humor ($p < 0.05$, $n = 6$).

GC and EGC were much higher in tissues. An exceptionally large volume of distribution, V_z, and oral clearance, Cl/F, of catechins in vitreous humor and plasma, for example, V_z of GC and GCG and Cl/F of GCG in plasma and V_z and Cl/F of ECG and ECGC in the humors, implied low selectivity of these catechins in those compartments (*24*). Radioactive [^{3}H]EGCG was found to be selectively absorbed into certain cells of various organs of mice (*27*).

The plasma was selective to non-gallate epimers. The vitreous humor appeared to be selective to nonepimers only (**Figure 2**). Aqueous humor and tissues exhibited no isomeric selectivity. Certain catechins were dominant in some compartments. For example, the relative AUC values of GC in vitreous humor and eye tissues and of C, GCG, and ECG in aqueous humor were >1 and even reaching 300-fold. There was likely selective tissue protein binding or active absorption.

Usually, the higher the exposure level of a drug, the slower is the elimination rate and the longer is the residence time. However, no relationship was found between AUC and λ_z or MRT_{inf} in any compartment except chloroid-sclera, where high correlation was found between AUC and MRT_{inf} (**Table 2**). Also, the AUC followed the chromatographic elution order with the most hydrophilic catechin, GC, having the highest AUC level and the least hydrophilic catechin, ECG, having the lowest AUC level. These suggest catechin retention follows hydrophilicity (**Table 2**).

The peak time, T_{max}, of the catechins in the eye can reflect the delivery pathway, presuming the flow followed the T_{max} length.

Table 2. Correlation Tests for Exposure Levels, AUC, from All Catechins against Their Elimination Rate λ_z and the AUC against Their Mean Residence Times, MRT_{inf}, in Each Compartment

	AUC vs λ_z				AUC vs MRT_{inf}			
	$y = ax + c$				$y = ax + c$			
	a	*c*	*R*	*p* value	*a*	*c*	*R*	*p* value
plasma	16910	−1794	0.7213	0.067	−332	3586	0.4428	0.32
aqueous humor	−4453	1524	0.5587	0.249	132.5	−949.4	0.7463	0.088
vitreous humor	3414	186	0.351	0.44	−54	1466	0.4852	0.2697
retina	−9532	21367	0.3397	0.576	2663	−11375	0.1488	0.8112
lens	−554	1846	0.356	0.488	39.5	1098	0.1526	0.773
cornea	−329	332	0.1686	0.749	−12	437	0.323	0.532
choroid-sclera	−32236	21270	0.5616	0.246	2703	−16024	0.9859	0.0003*[a]

[a] *, significant correlation ($p < 0.05$).

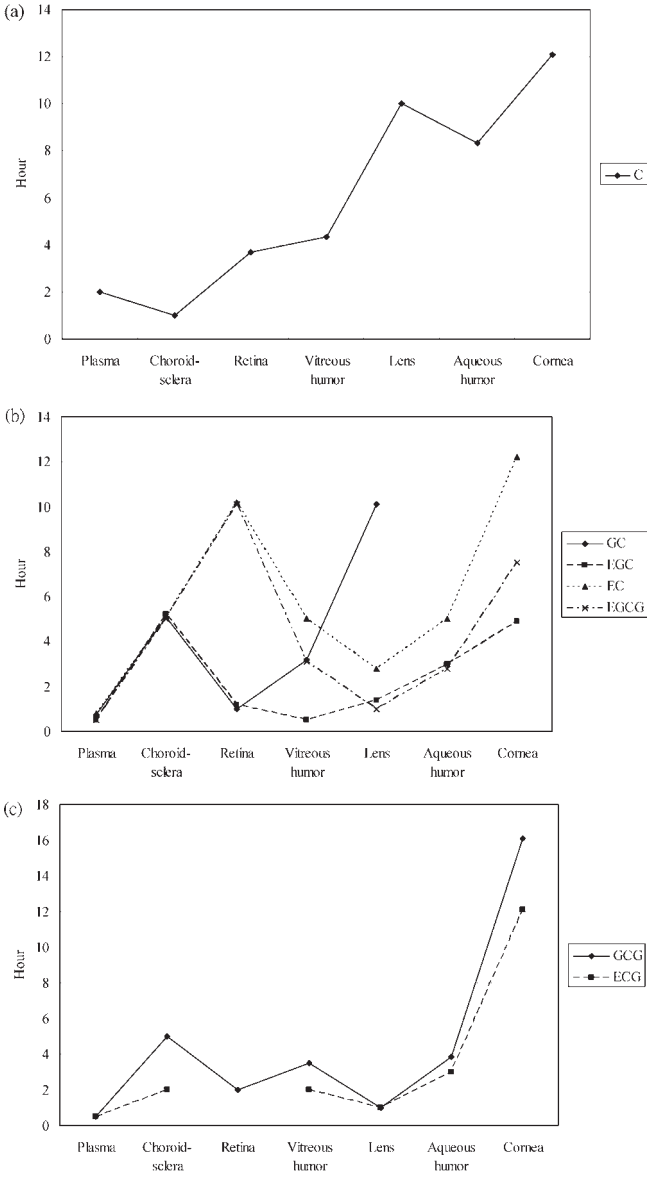

Figure 3. Three different general trends for the mean T_{max} values in catechins from plasma to different eye compartments: (**a**) general increasing trend from the plasma to the anterior segment; (**b**) middle puddle appearance; (**c**) roughly flat trend with abrupt rising in the anterior.

Although there was no clear unique pattern of T_{max} variation in the eye, there were three general trends of T_{max} of catechins in the humors and eye tissues (**Figure 3**). The first trend (**Figure 3a**) was a general increasing trend from the plasma to the anterior part of the eye. The catechin, C, may be delivered from the plasma through the outer region, posterior region to the anterior region, and finally reaching the cornea. The second trend (**Figure 3b**) demonstrated a middle puddle profile. It suggests the catechins EGCG and EC passed from the plasma through the capillaries of the inner eye to the ciliary body and the lens, then diverging to vitreous and aqueous humors, and finally reaching the retina and cornea. Or they may be delivered to the retina, as seen in EGC and

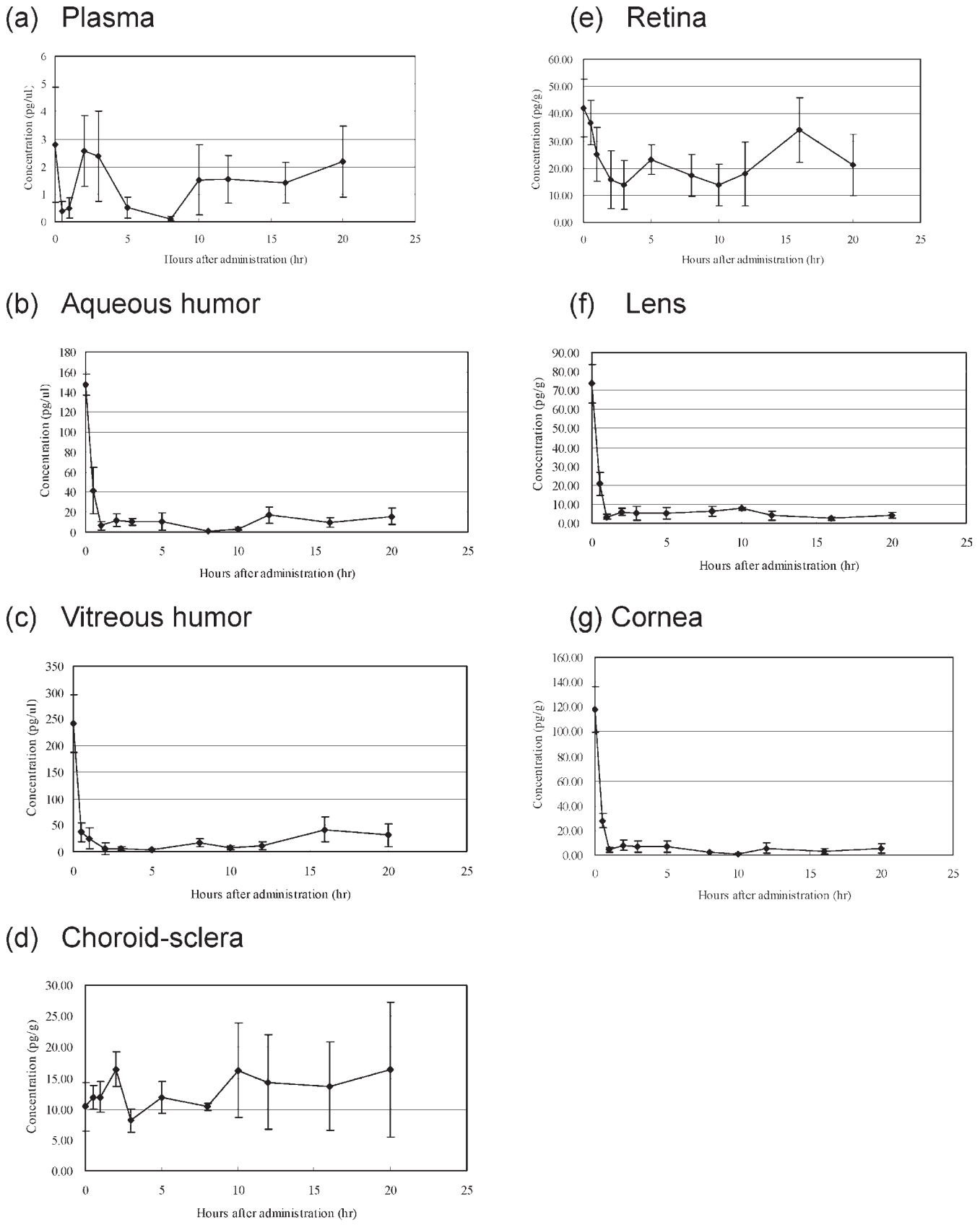

Figure 4. Profiles of 8-iso-$PGF_{2\alpha}$ in different compartments: (**a**) plasma; (**b**) aqueous humor; (**c**) vitreous humor; (**d**) choroid-sclera; (**e**) retina; (**f**) lens; (**g**) cornea. We compared 8-epi-isoprostane levels at time zero to the first minimum level. Panels **b**, **c**, **f**, and **g** show isoprostane levels in these regions rapidly and significantly reduced ($p < 0.001$, $n = 6$) and maintained at low level. Panel **e** shows isoprostane level slowly and significantly decreased to minimum level in retina ($p < 0.05$, $n = 6$) but was gradually increased again. No significant decrease in level was found in (**a**) plasma or (**d**) choroid-sclera. Error bars represent standard derivation.

GC, transfer through the choroid-sclera region, and enter the anterior part of the eye. Unfortunately, the level of GC was too low for determination in the aqueous humor and cornea. The third trend (**Figure 3c**) gave a platform in the posterior region and

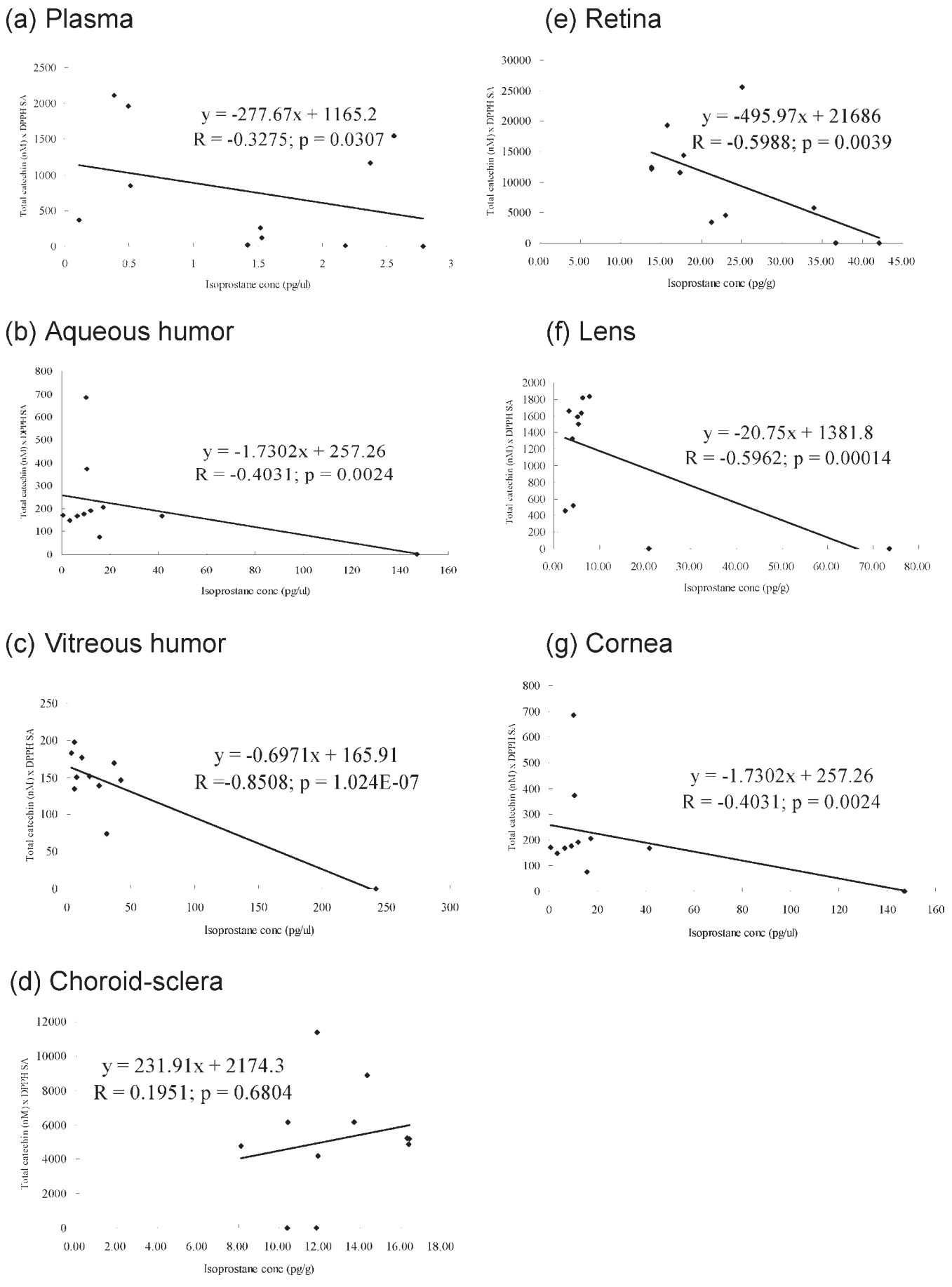

Figure 5. Correlation between total free radical scavenging activity of catechins with 8-isoprostane level in different compartments. All compartments showed significant correlation ($p < 0.05$) except choroid-sclera.

rose in the anterior part, which suggests the catechins GCG and ECG were evenly distributed to the posterior area by the capillaries in the chorioretinal region but cannot pass through the iris−lens barrier to the anterior part.

Many studies on the antioxidative effect of green tea focused on ECGC. However, in this study, we found its tissue level was not high. GC, EGC, C, and EC, on the other hand, substained high levels in many compartments. Although these compounds have a reducing power similar to or lower than that of EGCG (*28*), use of a mixture, such as GTE, was better than use of a single catechin because of lower cost and synergic effects on antioxidation and bioavailability (*24*, *28*).

Cherubini et al. (*29*) found that at least 5 μM polyphenols in human plasma was necessary to achieve significant protection against lipid peroxidation in vitro. In our study, only some catechins, such as GC and EGC, were above this level in the tissues (considering 1 g was equal to 1 mL). However, antioxidation was still effective according to the oxidative stress biomarker, 8-iso-$PGF_{2\alpha}$ (**Figure 4**). This may be due to the synergic effect of the different catechins. Quantum mechanics showed, among antioxidants, only catechins have a tunneling effect, which lowers the hydrogen donation activation energy and renders them effective free radical scavengers, with rapid neutralization even at low concentrations (*30*).

In general, the order of exposure level and C_{max} of catechins was retina > sclera > lens > cornea. Therefore, oral intake of GTE should provide effective antioxidant activity in the retina but less so in the cornea. However, our results demonstrated antioxidant activity was still found in the cornea according to the change in 8-isoprostane concentrations (**Figure 4g**). The oxidative stress levels of aqueous humor, vitreous humor, cornea, and lens were significantly reduced (**Figure 4b**,**c**,**f**,**g**), but it was significantly decreased only after 3 h in the retina and returned to normal levels afterward. No significant decrease in oxidative stress was in the plasma or choroid-sclera (**Figure 4a**,**e**). This could be explained by ocular physiology. Because the retina generates a lot of reactive species due to a high level of cellular metabolism, photochemical reactions, polyunsaturated fatty acid, and intense phagocytosis (*31*), high levels of antioxidative compounds including vitamin A, vitamin E, and carotenoids such as lutein and zeaxanthin are naturally present for protection (*32*).

There are strong negative correlations between the level of 8-isoprostane and the total free radical scavengeing activity from all catechins in each compartment (**Figure 5**) except the chloroid-sclera region. The total free radical scavenging activity is estimated by summation of the product of each catechin concentration and its corresponding DPPH-scavenging activity (*28*) in that compartment. Catechins may remove free radicals in each eye compartment except the chloroid-sclera region.

The oxidation stress of each tissue after catechin treatment was compared with time zero state. The oxidative stress depends on the basic metabolic status of the subject that has been maintained stably without significant diurnal variation of F_2-isoprostane in normal subjects (*33*, *34*). Therefore, we chose an initial point as a negative control reference for oxidative stress comparison to minimize the number of animals needed for sacrifice across the 11 time points according to the guideline of the Ethics Committee and the Federal Regulation for animal research (http://www.onlineethics.org/cms/16217.aspx). This baseline approach has been widely applied in many oxidative stress and antioxidant treatment studies (*35*, *36*).

In conclusion, catechins were differentially distributed and retained in the humors and eye tissues. The tissue exposure level in descending order was retina, choroid-sclera, lens, and cornea. The levels were higher in vitreous than in aqueous humor. The uptake of catechins might involve selective tissue binding or active absorption. Our dosage reduced oxidative stress in some eye tissues for up to 20 h. Our results indicate that green tea consumption could benefit the eye against oxidative stress.

ABBREVIATIONS USED

8-iso-$PGF2_{\alpha}$, 8-isoprostaglandin $F2_{\alpha}$; AUC, area under the curve; AUC_{inf}, area under the curve from zero time point to infinity; BHT, butylated hydroxytoluene; BSTFA, bis(trimethylsilyl)trifluoroacetamide; Cl/F, oral clearance; C, catechin; CG, catechin gallate; C_{max}, maximum concentration; EC, epicatechin; ECG, epicatechin gallate; EGC, epigallocatechin; EGCG, epigallocatechin gallate; GC, gallocatechin; GCG, gallocatechin gallate; MRT_{inf}, mean residence time from zero time point to infinity; PFBBr, pentafluorobenzyl bromide; TLC, thin layer chromatography; T_{max}, maximum peak time; V_z, volume of distribution; λ_z, terminal elimination rate.

ACKNOWLEDGMENT

We thank Taiyo Kagaku Co. Ltd for their generous donation of green tea extract tablets, Sunphenon DCF-1.

LITERATURE CITED

(1) Rafferty, N. S.; Rafferty, K. A.; Zigman, S. Comparative response to UV irradiation of cytoskeletal elements in rabbit and skate lens epithelial cells. *Curr. Eye Res.* **1997**, *16*, 310–319.

(2) Winkler, B. S.; Kapousta-Bruneau, N.; Arnold, M. J.; Green, D. G. Effects of inhibiting glutamine synthetase and blocking glutamate uptake on b-wave generation in the isolated rat retina. *Vis. Neurosci.* **1999**, *16*, 345–353.

(3) Liu, Q.; Ju, W. K.; Crowston, J. G.; Xie, F.; Perry, G.; Smith, M. A.; Lindsey, J. D.; Weinreb, R. N. Oxidative stress is an early event in hydrostatic pressure induced retinal ganglion cell damage. *Invest Ophthalmol. Vis. Sci.* **2007**, *48*, 4580–4589.

(4) Saccà, S. C.; Pascotto, A.; Camicione, P.; Capris, P.; Izzotti, A. Oxidative DNA damage in the human trabecular meshwork: clinical correlation in patients with primary open-angle glaucoma. *Arch. Ophthalmol.* **2005**, *123*, 458–463.

(5) Saugstad, O. D. Resuscitation of newborn infants with room air or oxygen. *Semin. Neonatol.* **2001**, *6*, 233–239.

(6) Brubaker, R. F.; Bourne, W. M.; Bachman, L. A.; McLaren, J. W. Ascorbic acid content of human corneal epithelium. *Invest. Ophthalmol. Vis. Sci.* **2000**, *41*, 1681–1683.

(7) Aydemir, O.; Celebi, S.; Yilmaz, T.; Yekeler, H.; Kükner, A. S. Protective effects of vitamin E forms (α-tocopherol, γ-tocopherol and *d*-α-tocopherol polyethylene glycol 1000 succinate) on retinal edema during ischemia-reperfusion injury in the guinea pig retina. *Int. Ophthalmol.* **2004**, *25*, 283–289.

(8) Kim, S. R.; Nakanishi, K.; Itagaki, Y.; Sparrow, J. R. Photooxidation of A2-PE, a photoreceptor outer segment fluorophore, protection by lutein and zeaxanthin. *Exp. Eye Res.* **2006**, *82*, 828–839.

(9) Khan, N.; Mukhtar, H. Tea polyphenols for health promotion. *Life Sci.* **2007**, *81*, 519–533.

(10) Kaszkin, M.; Beck, K. F.; Eberhardt, W.; Pfeilschifter, J. Unravelling green tea's mechanisms of action: more than meets the eye. *Mol. Pharmacol.* **2004**, *65*, 15–17.

(11) Zhang, B.; Osborne, N. N. Oxidative-induced retinal degeneration is attenuated by epigallocatechin gallate. *Brain Res.* **2006**, *1124*, 176–187.

(12) Chu, K. O.; Wang, C. C.; Chu, C. Y.; Chan, K. P.; Rogers, M. S.; Choy, K. W.; Pang, C. P. Pharmacokinetic studies of green tea catechins in maternal plasma and fetuses in rats. *J. Pharm. Sci.* **2006**, *95*, 1372–1381.

(13) Chu, K. O.; Wang, C. C.; Chu, C. Y.; Choy, K. W.; Pang, C. P.; Rogers, M. S. Uptake and distribution of catechins in fetal organs following in utero exposure in rats. *Hum. Reprod.* **2007**, *22*, 280–287.

(14) Morrow, J. D.; Roberts, L. J. The isoprostanes: unique bioactive products of lipid peroxidation. *Prog. Lipid Res.* **1997**, *36*, 1–21.

(15) Chen, L.; Lee, M. J.; Li, H.; Yang, C. S. Absorption, distribution, elimination of tea polyphenols in rats. *Drug Metab. Dispos.* **1997**, *25*, 1045–1050.

(16) Nakagawa, K.; Miyazawa, T. Absorption and distribution of tea catechin, (−)-epigallocatechin-3-gallate, in the rat. *J. Nutr. Sci. Vitaminol.* (*Tokyo*) **1997**, *43*, 679–684.

(17) Chu, K. O.; Wang, C. C.; Chu, C. Y.; Rogers, M. S.; Choy, K. W.; Pang, C. P. Determination of catechins and catechin gallates in tissues by liquid chromatography with coulometric array detection and selective solid phase extraction. *J. Chromatogr., B: Anal. Technol. Biomed. Life Sci.* **2004**, *810*, 187–195.

(18) Chu, K. O.; Wang, C. C.; Rogers, M. S.; Choy, K. W.; Pang, C. P. Determination of catechins and catechin gallates in biological fluids by HPLC with coulometric array detection and solid phase extraction. *Anal. Chim. Acta* **2004**, *510*, 69–76.

(19) Morrow, J. D.; Roberts, L. J.2nd. Mass spectrometric quantification of F2-isoprostanes in biological fluids and tissues as measure of oxidant stress. *Methods Enzymol.* **1999**, *300*, 3–12.

(20) Morrow, J. D.; Zackert, W. E.; Yang, J. P.; Kurhts, E. H.; Callewaert, D.; Dworski, R.; Kanai, K.; Taber, D.; Moore, K.; Oates, J. A.; Roberts, L. J.2nd Quantification of the major urinary metabolite of 15-F2t-isoprostane (8-iso-PGF2α) by a stable isotope dilution mass spectrometric assay. *Anal. Biochem.* **1999**, *269*, 326–331.

(21) Harada, M.; Kara, Y.; Naoki, H. Identification of antioxidative metabolites in biological fluid of the rat with ingested (+)-catechin and (−)-epicatechin. *Biosci., Biotechnol., Biochem.* **1999**, *63*, 973–977.

(22) Kida, K.; Suzuki, M.; Matsumoto, N.; Nanjo, F.; Hara, Y. Identification of biliary metabolites of (−)-epigallocatechin gallate in rats. *J. Agric. Food Chem.* **2000**, *48*, 4151–4155.

(23) Lambert, J. D.; Lee, M. J.; Lu, H.; Meng, X.; Hong, J. J.; Seril, D. N.; Sturgill, M. G.; Yang, C. S. Epigallocatechin-3-gallate is absorbed but extensively glucuronidated following oral administration to mice. *J. Nutr.* **2003**, *133*, 4172–4177.

(24) Chow, H. H.; Cai, Y.; Alberts, D. S.; Hakim, I.; Dorr, R.; Shahi, F.; Crowell, J. A.; Yang, C. S.; Hara, Y. Phase I pharmacokinetic study of tea polyphenols following single-dose administration of epigallocatechin gallate and polyphenon E. *Cancer Epidemiol. Biomarkers Prev.* **2001**, *10*, 53–58.

(25) Lin, L. C.; Wang, M. N.; Tseng, T. Y.; Sung, J. S.; Tsai, T. H. Pharmacokinetics of (−)-epigallocatechin-3-gallate in conscious and freely moving rats and its brain regional distribution. *J. Agric. Food Chem.* **2007**, *55*, 1517–1524.

(26) Hughes, P. M.; Olejnik, O.; Chang-Lin, J. E.; Wilson, C. G. Topical and systemic drug delivery to the posterior segments. *Adv. Drug Delivery Rev.* **2005**, *57*, 2010–2032.

(27) Suganuma, M.; Okabe, S.; Oniyama, M.; Tada, Y.; Ito, H.; Fujiki, H. Wide distribution of [3H](−)-epigallocatechin gallate, a cancer preventive tea polyphenol, in mouse tissue. *Carcinogenesis* **1998**, *19*, 1771–1776.

(28) Xu, J. Z.; Yeung, S. Y.; Chang, Q.; Huang, Y.; Chen, Z. Y. Comparison of antioxidant activity and bioavailability of tea epicatechins with their epimers. *Br. J. Nutr.* **2004**, *91*, 873–881.

(29) Cherubini, A.; Beal, M. F.; Frei, B. Black tea increases the resistance of human plasma to lipid peroxidation *in vitro*, but not ex vivo. *Free Radical Biol. Med.* **1999**, *27*, 381–387.

(30) Tejero, I.; Gonzalez-Garcia, N.; Gonzalez-Lafont, A.; Lluch, J. M. Tunneling in green tea: understanding the antioxidant activity of catechol-containing compounds. A variational transition-state theory study. *J. Am. Chem. Soc.* **2007**, *129*, 5846–5854.

(31) Miceli, M. V.; Liles, M. R.; Newsome, D. A. Evaluation of oxidative processes in human pigment epithelial cells associated with retinal outer segment phagocytosis. *Exp. Cell Res.* **1994**, *214*, 242–249.

(32) Trevithick-Sutton, C. C.; Foote, C. S.; Collins, M.; Trevithick, J. R. Retinal carotenoids zeaxanthin and lutein scavenge superoxide and hydroxyl radicals: a chemiluminescence and ESR study. *Mol. Vis.* **2006**, *12*, 1127–1135.

(33) Helmersson, J.; Basu, S. F2-isoprostane excretion rate and diurnal variation in human urine. *Prostaglandins, Leukotrienes Essent. Fatty Acids* **1999**, *61*, 203–205.

(34) Ogawa, F.; Shimizu, K.; Muroi, E.; Hara, T.; Hasegawa, M.; Takehara, K.; Sato, S. Serum levels of 8-isoprostane, a marker of oxidative stress, are elevated in patients with systemic sclerosis. *Rheumatology* **2006**, *45*, 815–818.

(35) Hanwell, H. E.; Kay, C. D.; Lampe, J. W.; Holub, B. J.; Duncan, A. M. Acute fish oil and soy isoflavone supplementation increase postprandial serum (n-3) polyunsaturated fatty acids and isoflavones but do not affect triacylglycerols or biomarkers of oxidative stress in overweight and obese hypertriglyceridemic men. *J. Nutr.* **2009**, *139*, 1128–1134.

(36) Patel, M.; Liang, L. P.; Roberts, L. J.2nd. Enhanced hippocampal F2-isoprostane formation following kainate-induced seizures. *J. Neurochem.* **2001**, *79*, 1065–1069.

Received for review September 17, 2009. Revised manuscript received December 1, 2009. Accepted January 05, 2010. This study was supported by the Hong Kong Special Administration Region Research Grant Council (CUHK4077/01M).